Electrochemistry

Received: October 31, 2017
Accepted: February 19, 2018
Published online: April 5, 2018

The Electrochemical Society of Japan

https://doi.org/10.5796/electrochemistry.17-00082

Article

Electrochemistry, **86(2)**, 99–103 (2018)

Electrochemical Behavior of Ti(III) Ions in a KF–KCl Eutectic Melt

Yutaro NORIKAWA,[a] Kouji YASUDA,[b,c] and Toshiyuki NOHIRA[a,*]

[a] *Institute of Advanced Energy, Kyoto University, Gokasho, Uji, Kyoto 611-0011, Japan*
[b] *Agency for Health, Safety and Environment, Kyoto University, Yoshida-hommachi, Sakyo-ku, Kyoto 606-8501, Japan*
[c] *Department of Fundamental Energy Science, Graduate School of Energy Science, Kyoto University, Yoshida-hommachi, Sakyo-ku, Kyoto 606-8501, Japan*

* *Corresponding author: t-nohira@iae.kyoto-u.ac.jp*

ABSTRACT

The electrochemical behavior of Ti(III) ions in a eutectic KF–KCl molten salt was investigated using cyclic voltammetry, square wave voltammetry, and chronoamperometry at 923 K. Ti(III) ions were produced by the addition of 0.50 mol% of K_2TiF_6 and 0.33 mol% of Ti sponge to the melt. The reduction of Ti(III) ions to metallic Ti was observed as a single 3-electron wave around 0.33 V vs. K^+/K in the square-wave voltammogram. The electrodeposition was conducted at a Mo electrode by galvanostatic electrolysis at $-50\,mA\,cm^{-2}$ for 20 min. The deposits were confirmed to be compact and adherent Ti metal films by scanning electron microscopy, energy dispersive X-ray analysis and X-ray diffraction analysis. The oxidation of Ti(III) to Ti(IV) was observed at 1.82 V vs. K^+/K as a reversible electrochemical process. The diffusion coefficient of Ti(III) ions was determined to be $3.9 \times 10^{-5}\,cm^2\,s^{-1}$.

Keywords : Titanium, Molten Salt, Electrodeposition, KF–KCl

1. Introduction

Titanium metal has many attractive properties such as a high strength-to-weight ratio, corrosion resistance, heat resistance and biocompatibility. Owing to these properties, Ti metal is an indispensable material for aircrafts, chemical plants, etc. However, compared with iron and aluminum, widespread use of Ti has not been realized because of its high production cost and poor workability. Thus, the development of a new manufacturing process for Ti is required to increase its utilization.

Plating metallic Ti on general substrates is one of the most practical methods to utilize the superior properties of Ti. Electrodeposition is one of the promising Ti plating methods due to expected high deposition rate and low cost. Further, plating on substrates with complicated shapes is possible with electrodeposition. Electrodeposition of Ti metal has been investigated using high-temperature molten salts, such as chlorides, fluorides, and chloride–fluoride mixtures.[1–19] In chloride melts, compact and smooth Ti films were difficult to obtain.[1–10] On the other hand, in fluoride melts, compact and smooth Ti films were obtained in LiF–NaF–KF melts by Robin et al. at 873–923 K[11,12] and by Lepinay et al. at 823–1023 K.[13] In chloride–fluoride mixtures, Wei et al. obtained compact and smooth Ti films in LiCl–NaCl–KCl containing K_2TiF_6 at 723–923 K.[14] Ene and Zuca reported a similar result in NaCl–KCl containing K_2TiF_6.[15] Compact and smooth films were also electrodeposited by Barner et al. in NaCl–KCl–NaF at 973 K[16] and by Malyshev and Shakhnin in KCl–NaCl–NaF–$TiCl_3$ at 1073 K.[17] Takamura et al. reported an improvement of the morphology of deposits by addition of LiF to LiCl–KCl at 773 K.[18] According to Song et al., Ti metal with fine crystal grains was obtained when KF was added to KCl–NaCl at 1073 K.[19] To summarize, compact and smooth Ti films have been obtained using fluoride-based melts and fluoride-added melts. However, the major problem with the use of fluoride-based molten salts is removing the adhered salts on the Ti films. Since most fluoride salts have low solubility in water (LiF: 0.13, NaF: 4.15, MgF_2: 0.13, CaF_2: 0.0016 g (per 100 g H_2O)),[20] water washing does not effectively remove them from the Ti films.

From the background above, we have proposed a new electrodeposition process for Ti using KF–KCl as a molten salt electrolyte.[21,22] Among alkali metal and alkaline earth fluorides, KF has exceptionally high solubility in water (101.6 g per 100 g H_2O)).[20] However, using only KF molten salt is impractical due to its high melting point (1131 K). Since KCl also has high solubility in water (35.9 g per 100 g H_2O),[20] a lower melting point and easy removal of solidified salts can be achieved using the KF–KCl binary melt (melting point = 878 K at the eutectic composition KF:KCl = 45:55 mol%[23]).

The electrochemical reduction mechanism of Ti(IV) ions has also been reported by various researchers. In molten LiF–NaF–KF and LiF–KF at 823–1023 K,[11–13,24] the deposition of Ti metal from Ti(IV) ions was reported to occur in two reduction steps because of the high stability of Ti(III) and Ti(IV) ions. In the fluoride melts, the Ti ions were considered to exist as complexes with fluoride ions. Compact and smooth Ti films were obtained when the Ti ions were controlled to be only in an oxidation state of +3. The influence of the addition of fluoride ions into chloride melts on the valence of Ti ions has also been investigated. Guangsen et al. reported that electrodeposition of Ti metal occurred in two reduction steps from Ti(IV) when the amounts of KF added exceeded 10 wt% into NaCl–KCl–K_2TiF_6 (3 wt%).[25] The stability of Ti-halide complexes changed depending on the concentration of fluoride ions, which affected the electrochemical reduction mechanism.

In this study, the electrochemical behavior of Ti(III) ions was investigated in a KF–KCl eutectic melt at 923 K to obtain fundamental data concerning this molten salt system. Cyclic voltammetry and square wave voltammetry were conducted to analyze the cathodic and the anodic reactions of Ti(III) ions. Furthermore, the diffusion coefficient of Ti(III) ions was evaluated using cyclic voltammetry and chronoamperometry.

2. Experimental

Reagent-grade KF (Wako Pure Chemical Co., Ltd., >99.0%) and KCl (Wako Pure Chemical Co., Ltd., >99.5%) were mixed to the

eutectic composition (molar ratio of KF:KCl = 45:55, melting point = 878 K,[23] 400 g) and were loaded in a Ni crucible (Chiyoda Industry Co., Ltd., outer diameter: 96 mm, height: 102 mm). The mixture in the crucible was first dried under vacuum at 453 K for 72 h. The crucible was placed at the bottom of a stainless-steel vessel in an air-tight Kanthal container and further dried under vacuum at 773 K for 24 h. The electrochemical measurements were conducted in a dry Ar atmosphere at 923 K in a glove box. After blank measurements in KF–KCl, 0.50 mol% of K_2TiF_6 (Morita Chemical Industry Co., Ltd., >97.5%) and 0.33 mol% of Ti sponge (Wako Pure Chemical Co., Ltd., >99%) were added to the melt. Here, 0.33 mol% of Ti sponge corresponds to approximately twice the amount necessary to generate Ti(III) ions from 0.50 mol% of K_2TiF_6 according to Eq. (1).

$$\mathrm{Ti(0)} + 3\mathrm{Ti(IV)} \rightarrow 4\mathrm{Ti(III)} \quad (1)$$

Electrochemical measurements and galvanostatic electrolysis were conducted using a three-electrode method with an electrochemical measurement system (Hokuto Denko Corp., HZ-7000). The working electrodes were Mo plate (Nilaco Corp., 5 mm × 10 mm, thickness: 0.1 mm, 99.95%), Mo flag (Nilaco Corp., diameter: 2.0 mm, thickness: 0.1 mm, 99.95%), and Pt flag (Nilaco Corp., diameter: 2.0 mm, thickness: 0.1 mm, 99.98%) electrodes. The structure of the flag electrodes was reported in our previous paper.[26] Prior to the experiments, the Mo and Pt electrodes were washed with ethanol and well dried. A Ti plate (Nilaco Corp., 5 mm × 10 mm, thickness: 0.1 mm, 99.5%) was used as the counter electrode. A Ti rod (Nilaco Corp., diameter: 3.0 mm, 99.5%) was employed as a reference electrode. The potential of reference electrode was calibrated with reference to a dynamic K^+/K potential estimated by cyclic voltammetry on the Mo flag.[26] The melt temperature was measured using a type-K thermocouple. The electrolyzed samples on the Mo plates were soaked in distilled water at 333 K for 10 min to remove the salt adhered on the deposits.

The surface and cross-section of the sample were observed by scanning electron microscopy (SEM; Keyence Corp., VE-8800). Before the observation of the cross section, the samples were embedded in acrylic resin and polished with emery papers and buffing compounds. Then, the samples were coated with Au using an ion sputtering apparatus (Hitachi, Ltd., E-1010) to give conductivity. The deposits were also characterized by energy-dispersive X-ray (EDX; AMETEK Co., Ltd., EDAX Genesis APEX2) and X-ray diffraction (XRD; Rigaku Corp., Ultima IV, Cu-*Kα* line) analyses. A small portion of molten salt was sampled and dissolved in a 10 wt% HF aq. solution. The solution was analyzed by inductively coupled plasma atomic emission spectroscopy (ICP-AES; Hitachi, Ltd., SPECTRO BLUE) to determine the Ti ion concentration in molten salt.

3. Result and Discussion

3.1 Cathodic reduction of Ti(III) ions

3.1.1 Cyclic voltammetry

Figure 1 shows the cyclic voltammogram in the negative potential region obtained at the Mo flag electrode after the addition of 0.50 mol% of K_2TiF_6 and 0.33 mol% of Ti sponge at a temperature of 923 K and a scan rate of 0.50 V s^{-1}. For comparison, the voltammogram before the addition is also plotted. From approximately 0.4 V (vs. K^+/K), cathodic current (A) is observed, which possibly corresponds to electrodeposition of Ti metal. After reversing the scanning direction, anodic current (A′) is also observed, which is considered to be due to anodic dissolution of Ti metal.

3.1.2 Galvanostatic electrolysis, XRD and SEM/EDX

To confirm whether the cathodic current (A) corresponds to Ti metal deposition, galvanostatic electrolysis was conducted using the

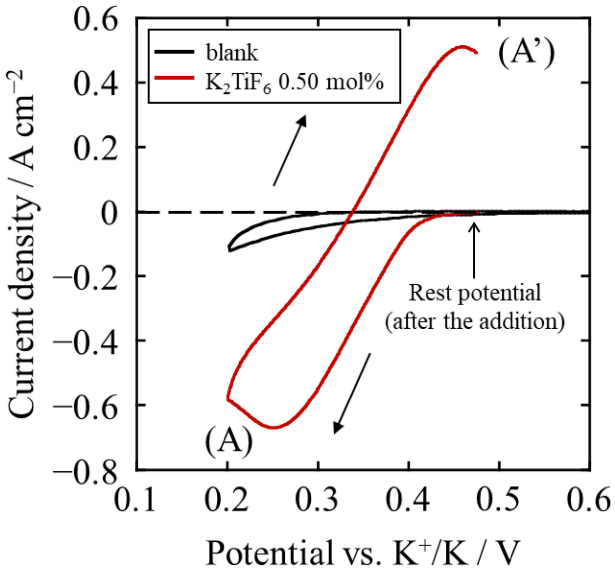

Figure 1. Cyclic voltammograms at the Mo flag electrode in molten KF–KCl before and after the addition of K_2TiF_6 (0.50 mol%) and sponge Ti (0.33 mol%) at 923 K. Scan rate: 0.50 V s^{-1}.

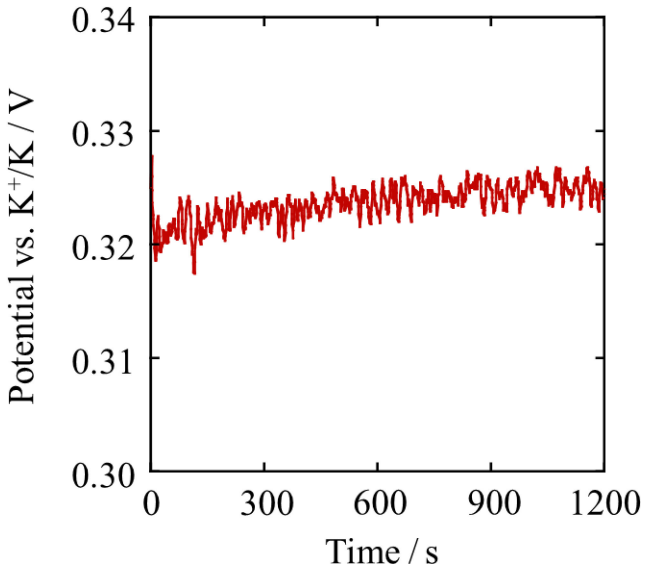

Figure 2. Potential transient curve during the galvanostatic electrolysis at the Mo plate electrode at −50 mA cm^{-2} for 20 min in KF–KCl after the addition of K_2TiF_6 (0.50 mol%) and sponge Ti (0.33 mol%) at 923 K.

Mo plate electrode at a current density of −50 mA cm^{-2} for 20 min. Figure 2 shows the potential transient curve during the galvanostatic electrolysis. The potential during the electrolysis is around 0.32 V, which indicates the progress of the cathodic reaction observed in the cyclic voltammogram. Figure 3(a) shows an optical image of the sample after washing in water. The entirety of the substrate is covered in a deposit with a metallic luster. Figure 3(b) shows an XRD pattern of the sample, which clearly indicates the existence metallic Ti. Surface and cross-sectional SEM images of the sample are shown in Figs. 4(a) and (b), respectively. The deposit is compact and composed of grains with diameters of approximately 10 µm. EDX analysis of the deposit detected only Ti. The cross-sectional SEM image confirms that adherent and smooth films with thickness of 20 µm are electrodeposited on the Mo substrate. From these

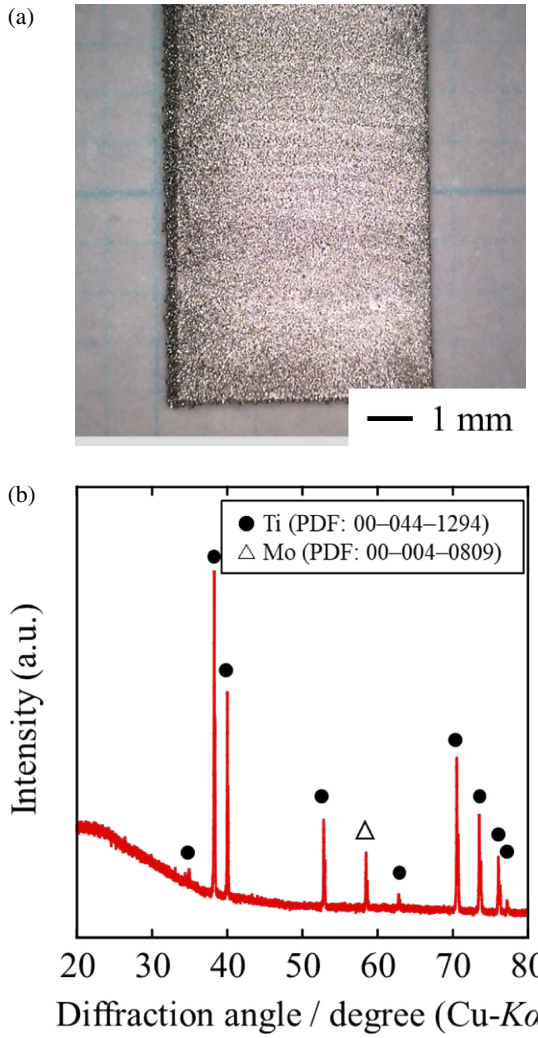

Figure 3. (a) Optical image and (b) XRD pattern of the sample obtained by galvanostatic electrolysis at the Mo plate electrode at $-50\,\mathrm{mA\,cm^{-2}}$ for 20 min in molten KF–KCl after the addition of K_2TiF_6 (0.50 mol%) and sponge Ti (0.33 mol%) at 923 K.

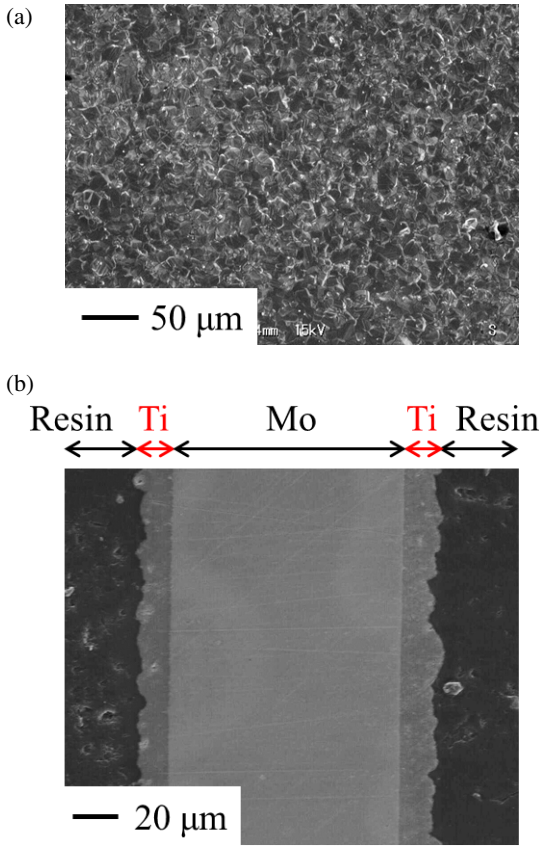

Figure 4. (a) Surface and (b) cross-sectional SEM images of the sample obtained by galvanostatic electrolysis at the Mo plate electrode at $-50\,\mathrm{mA\,cm^{-2}}$ for 20 min in molten KF–KCl after the addition of K_2TiF_6 (0.50 mol%) and sponge Ti (0.33 mol%) at 923 K.

results, the cathodic wave in the cyclic voltammogram is assigned to the reduction of Ti(III) ions to metallic Ti.

3.1.3 Square wave voltammetry

For more detailed analysis of the cathodic reaction, square wave voltammetry was conducted in the same melt. In a square wave voltammogram, the half width of a peak, $W_{1/2}$, is given by Eq. (2).[27,28]

$$W_{1/2} = 3.53RT/nF \qquad (2)$$

Here, R is the gas constant, T is the temperature, n is the number of electrons transferred, and F is the Faraday constant. Figure 5 shows the square wave voltammogram obtained at a frequency of 5 Hz, in which the background current correction has been conducted. A fitted curve using the Gaussian function is also plotted. The voltammogram exhibits a single peak with a half width of 90 mV. The peak potential is observed at 0.33 V, corresponding to the potential at which cathodic current sharply increases in the cyclic voltammogram. The background corrected voltammogram deviates from the fitted curve around 0.4 V, which may be the result of the formation of a solid solution of Ti in Mo. In the potential region more negative than 0.3 V, the voltammogram also deviates from the fitted curve, which is explained by the increase of electrode area due to nucleation and growth of Ti. The number of transferred electrons is calculated to be 3.1 from the peak half width. Thus, the cathodic

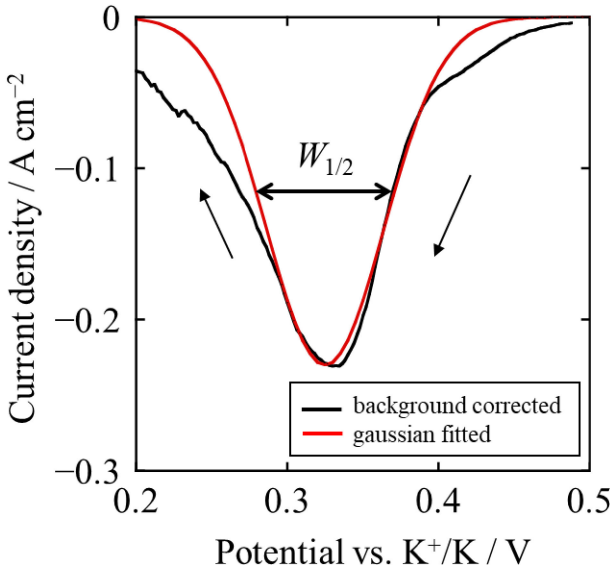

Figure 5. Square wave voltammogram at the Mo flag electrode in molten KF–KCl after the addition of K_2TiF_6 (0.50 mol%) and sponge Ti (0.33 mol%) at 923 K. Frequency: 5 Hz.

current peak at 0.33 V is reasonably interpreted as the reduction of Ti(III) ions to Ti metal. This result also indicates that Ti(II) ions are not formed in KF–KCl molten salt. Guangsen et al. also reported that Ti(II) ions disappeared in NaCl–KCl–K_2TiF_6 (3 wt%) melts at 973 K when the added amounts of KF exceeded 10 wt%.[25]

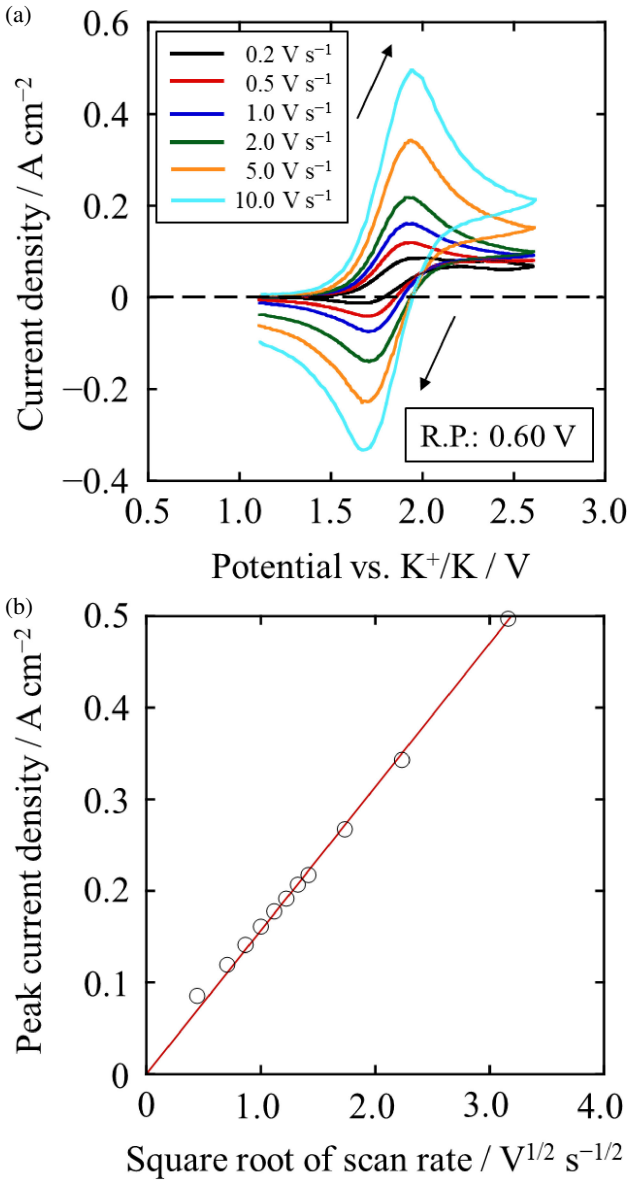

Figure 6. (a) Cyclic voltammograms at the Pt flag electrode in molten KF–KCl after the addition of K_2TiF_6 (0.50 mol%) and sponge Ti (0.33 mol%) at various scan rates at 923 K. (b) Dependence of anodic peak current density on scan rate.

3.2 Anodic oxidation of Ti(III) ions

3.2.1 Cyclic voltammetry

Figure 6(a) shows the cyclic voltammograms obtained at the Pt flag electrode in the positive potential region. The scan rates were varied from 0.20 V s^{-1} to 10 V s^{-1} with 60% in-situ IR compensation. At each scan rate, a pair of redox current peaks is observed at around 1.8 V. This redox reaction is considered a reversible process because the peak potential is constant regardless of scan rate. For a reversible reaction, the following relationship holds between the anodic peak potential (E_{ap}) and the cathodic peak potential (E_{cp}),[29]

$$E_{ap} - E_{cp} \cong 2.3RT/nF. \quad (3)$$

Since the difference of peak potential in Fig. 6(a) is 0.20 V, the number of transferred electrons is calculated to be 0.91 by Eq. (3). Thus, the redox reaction around 1.8 V corresponds to the redox reaction of Ti(III)/Ti(IV).

Further, the concentration ratio of Ti(III) to Ti(IV) ions was calculated. The equilibrium potential of Ti(III)/Ti(IV) redox reaction, E, is determined by Nernst equation (Eq. (4)).

$$E = E^{\circ\prime} - \frac{RT}{F} \ln \frac{c_{Ti(III)}}{c_{Ti(IV)}} \quad (4)$$

Here, $E^{\circ\prime}$ is the standard formal redox potential, and $c_{Ti(III)}$ and $c_{Ti(IV)}$ are concentrations of Ti(III) and Ti(IV) ions, respectively. In the present experiment, E was measured to be 0.60 V from the rest potential of the Pt electrode which was considered to be determined by the equilibrium potential of Ti(III)/Ti(IV) redox reaction. The value of $E^{\circ\prime}$ is calculated to be 1.82 V from the averaged value of E_{ap} and E_{cp} from the cyclic voltammogram.[29] Thus, the concentration ratio of Ti(III) to Ti(IV) ions is calculated to be 4.6×10^6, which confirms that almost all Ti(IV) ions were transformed to Ti(III) ions by the comproportionation reaction of Eq. (1).

3.2.2 Determination of diffusion coefficient of Ti(III) ions by cyclic voltammetry and chronoamperometry

The diffusion coefficient of Ti(III) ions in KF–KCl molten salt was determined by the obtained cyclic voltammograms in Fig. 6. When a reaction is reversible and both the reactants and products are soluble, the anodic peak current (I_{ap}) is given by Eq. (5).

$$I_{ap} = 0.446FAc_{Ti(III)}(D_{Ti(III)}Fv/RT)^{1/2}, \quad (5)$$

Here, A is the electrode area, $D_{Ti(III)}$ is the diffusion coefficient of Ti(III) ions, and v is the scan rate. The volume concentration of ions in the electrolyte, $c_{Ti(III)}$, is calculated using the density of the KF–KCl melt (KF:KCl = 45:55 mol%, $\rho = 1.74$ g cm^{-3} at 923 K). The density is estimated by an extrapolation of the reported data for the KF:KCl compositions of 37:63 and 50:50 mol% in the temperature range of 1050–1250 K.[30] Figure 6(b) shows the plots of anodic peak current densities against the square roots of the scan rates. From Eq. (5) and the slope of the plots, the value of $D_{Ti(III)}$ is determined to be 3.4×10^{-5} cm^2 s^{-1} at 923 K.

The diffusion coefficient of Ti(III) was also measured by chronoamperometry. When the rate determining step is the diffusion of ions, the current-time response follows the Cottrell equation.[31] The current, I, is proportional to the reciprocal of the square root of time, t.

$$I = \frac{FAD_{Ti(III)}{}^{1/2}c_{Ti(III)}}{\pi^{1/2}t^{1/2}} \quad (6)$$

The value of $D_{Ti(III)}$ can be determined from the slope of the plot of the current density versus the reciprocal of the square root of time.

For the evaluation, the potential should be set in the mass-transfer-limited region. Thus, 2.3 V and 2.4 V were selected because they were more positive than the peak potential for Ti(III) oxidation, as obtained from the cyclic voltammogram. Figure 7(a) shows the chronoamperograms at the Pt flag electrode. The two chronoamperograms overlap and the anodic current densities asymptotically approach 0.10 A cm^{-2} after two seconds, indicating a diffusion-limited current. Figure 7(b) shows the relationship between the current density and the reciprocal of the square root of time. Both the plots of 2.3 V and 2.4 V have a proportional relation in the range of $3 < t^{-1/2} < 6$. At small $t^{-1/2}$ values, the observed relationship deviates from the Cottrell equation because the growth of diffusion layer is not infinite. From the data in the range of $3 < t^{-1/2} < 6$, the diffusion coefficient of Ti(III) ions at 923 K is calculated to be 3.9×10^{-5} cm^2 s^{-1}. The diffusion coefficient obtained by cyclic voltammetry is smaller than the one obtained by chronoamperometry. Although in-situ IR compensation was conducted in cyclic voltammetry, the highest compensation ratio without potential instability was 60%. Thus, the actual potential sweep rates were lower than the specified ones due to IR drops, which explains the smaller diffusion coefficient. Considering this, the value obtained by chronoamperometry, 3.9×10^{-5} cm^2 s^{-1}, should be more accurate. The value is 1.4-times larger than the reported value of 2.7×10^{-5} cm^2 s^{-1} in molten LiF–NaF–KF at 973 K,[11] which is likely due to the difference in the viscosities of the molten salts.

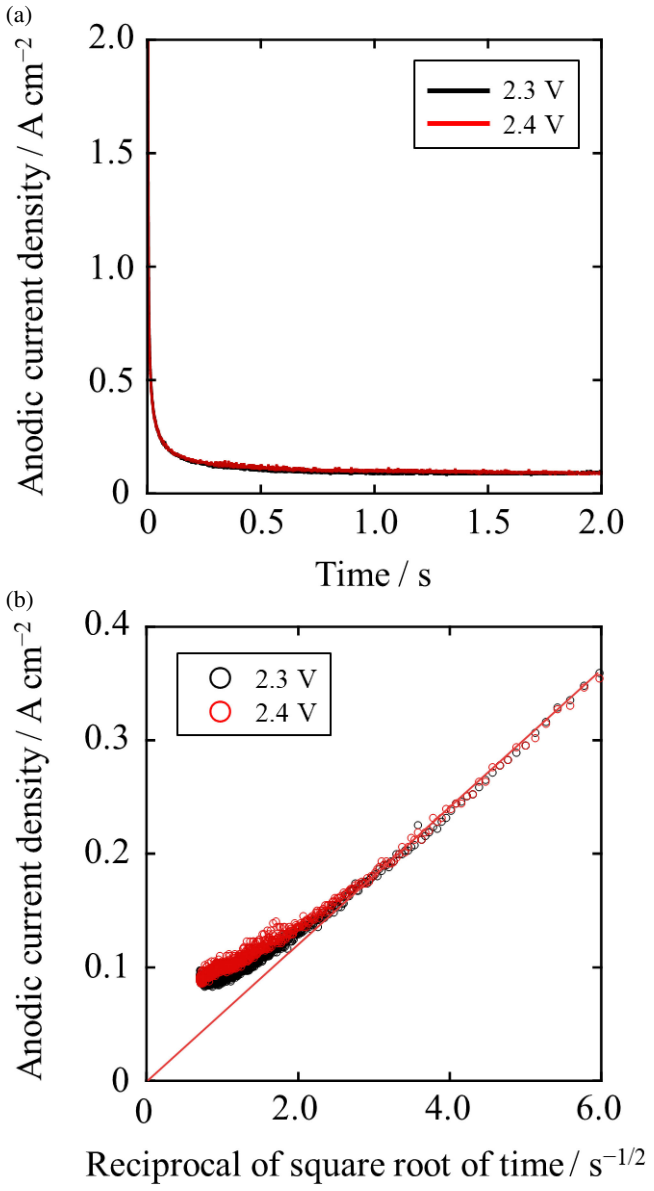

Figure 7. (a) Chronoamperograms at the Pt flag electrode at 2.3 V and 2.4 V in molten KF–KCl after the addition of K_2TiF_6 (0.50 mol%) and sponge Ti (0.33 mol%) at 923 K. (b) Relationship of the current density and the reciprocal of square root of time.

4. Conclusion

The electrochemical behavior of Ti(III) ions was investigated in the KF–KCl eutectic melt after the addition of 0.50 mol% of K_2TiF_6 and 0.33 mol% of Ti sponge at 923 K. The cathodic reaction around 0.33 V (vs. K^+/K) was determined to be the reduction of Ti(III) ions to Ti metal from the results of cyclic voltammetry, square wave voltammetry, and SEM/EDX and XRD analyses of the deposits. The anodic reaction around 1.82 V in cyclic voltammetry was found to be the electrochemically reversible oxidation of Ti(III) ions to Ti(IV) ions. The completion of the comproportionation reaction from Ti(IV) and Ti(0) to Ti(III) was confirmed by the calculation of the concentration ratio of Ti(III) to Ti(IV). The diffusion coefficient of Ti(III) ions at 923 K was determined to be 3.9×10^{-5} cm^2 s^{-1} by chronoamperometry.

Acknowledgments

Part of this study was conducted as collaborative research with Sumitomo Electric Industries, Ltd.

References

1. M. B. Alpert, F. J. Schultz, and W. F. Sullivan, *J. Electrochem. Soc.*, **104**, 555 (1957).
2. B. J. Fortin, J. G. Wurm, L. Gravel, and R. J. A. Potvin, *J. Electrochem. Soc.*, **106**, 428 (1959).
3. J. A. Menzies, D. L. Hill, G. J. Hills, L. Young, and J. O'M. Bockris, *J. Electroanal. Chem.*, **1**, 161 (1959).
4. G. M. Haarberg, W. Rolland, A. Sterten, and J. Thonstad, *J. Appl. Electrochem.*, **23**, 217 (1993).
5. H. Takamura, I. Ohno, and H. Numata, *J. Jpn. Inst. Metals*, **60**, 388 (1996).
6. J. G. Gussone and J. M. Hausmann, *J. Appl. Electrochem.*, **41**, 657 (2011).
7. X. Ning, H. Asheim, H. Ren, S. Jiao, and H. Zhu, *Metall. Mater. Trans. B*, **42**, 1181 (2011).
8. Y. Song, S. Jiao, L. Hu, and Z. Guo, *Metall. Mater. Trans. B*, **47**, 804 (2016).
9. T. Uda, T. H. Okabe, Y. Waseda, and Y. Awakura, *Sci. Technol. Adv. Mater.*, **7**, 490 (2006).
10. M. H. Kang, J. Song, H. Zhu, and S. Jiao, *Metall. Mater. Trans. B*, **46**, 162 (2015).
11. A. Robin, J. D. Lepinay, and M. J. Barbier, *J. Electroanal. Chem.*, **230**, 125 (1987).
12. A. Robin and R. B. Ribeiro, *J. Appl. Electrochem.*, **30**, 239 (2000).
13. J. D. Lepinay, J. Bouteillon, S. Traore, D. Renaud, and M. J. Barbier, *J. Appl. Electrochem.*, **17**, 294 (1987).
14. D. Wei, M. Okido, and T. Oki, *J. Appl. Electrochem.*, **24**, 923 (1994).
15. N. Ene and S. Zuca, *J. Appl. Electrochem.*, **25**, 671 (1995).
16. J. H. Barner, P. Noye, A. Barhoun, and F. Lantelme, *J. Electrochem. Soc.*, **152**, C20 (2005).
17. V. V. Malyshev and D. B. Shakhnin, *Mater. Sci.*, **50**, 80 (2014).
18. H. Takamura, I. Ohno, and H. Numata, *J. Jpn. Inst. Metals*, **60**, 388 (1996).
19. J. Song, Q. Wang, X. Zhu, J. Hou, S. Jiao, and H. Zhu, *Mater. Trans.*, **55**, 1299 (2014).
20. *Rikagaku Jiten, 4th Edition* (Eds. R. Kubo, S. Nagakura, H. Iguchi, and H. Ezawa), Iwanami Shoten, Publishers, Tokyo (1987). [in Japanese]
21. Y. Norikawa, K. Yasuda, and T. Nohira, *Mater. Trans.*, **58**, 390 (2017).
22. Y. Norikawa, K. Yasuda, and T. Nohira, *Proceedings of 6th Asian Conference on Molten Salts Chemistry and Technology (AMS6)*, Gyeongju, Korea, 13–16 June, 2017, OA07 (2017).
23. *Phase Diagrams for Ceramists Vol. VII* (Eds. L. P. Cook and H. F. McMurdie), The American Ceramic Society Inc., Columbus, p. 509 (1989).
24. F. R. Clayton, G. Mamantov, and D. L. Manning, *J. Electrochem. Soc.*, **120**, 1993 (1973).
25. C. Guangsen, M. Okido, and T. Oki, *J. Appl. Electrochem.*, **18**, 80 (1988).
26. K. Maeda, K. Yasuda, T. Nohira, R. Hagiwara, and T. Homma, *J. Electrochem. Soc.*, **162**, D444 (2015).
27. L. Ramaley and M. S. Krause, *Anal. Chem.*, **41**, 1362 (1969).
28. M. S. Krause and L. Ramaley, *Anal. Chem.*, **41**, 1365 (1969).
29. R. S. Nicholson and I. Shain, *Anal. Chem.*, **36**, 706 (1964).
30. G. J. Janz, *J. Phys. Chem. Ref. Data*, **17**, 42 (1988).
31. F. G. Cottrell, *Z. Phys. Chem.*, **42**, 385 (1902).